Optimisation of Contact Parameters of Unidirectional FRP Composite Bearings

Thyla, P.R.[1] and Gomathinayagam, A.[2]
[1]Assistant Professor Department of Mechanical Engineering PSG College of Technology Coimbatore – 641 004.
[2]Assistant Manager – Design Product Development Centre Larsen & Tubro Ltd Coimbatore

Received on 20/03/2010; Accepted on 19/06/2010

Abstract
The contact characteristics of unidirectional continuous fiber-reinforced plastic (FRP) composite bearings are investigated based on Hwu and Fan's closed form analytical solution. The particular condition of a rigid parabolic cylinder in frictional sliding contact with the composite is evaluated. The influences of sliding direction, fiber material, matrix material, fiber volume fraction and fiber ply orientation on the surface contact pressure are determined and compared with published results. From the analytical results, several important trends for the contact behavior of FRP composite bearings are discussed. The contact parameters for unidirectional FRP composite bearings are optimized using genetic algorithm. The study shows that, in case of unidirectional FRP composite bearings, the highest maximum contact pressure is obtained in the normal direction and hence, the normal direction has the highest wear resistance. It is also observed that increasing the volume fraction of fibers increases the maximum contact pressure in all the three directions. The transverse and parallel directions are least sensitive to the fiber ply orientation, whereas the normal direction shows a considerable change in the maximum contact pressure, contact patch and symmetry parameter with a variation of the fiber ply orientation. With regard to crossply FRP composite bearings, it is found that the contact pressure distribution and the contact patch are same for the transverse and parallel directions. These bearings have more strength along the transverse and parallel directions and less strength along the normal direction *t* the unidirectional bearings.

NOMENCLATURE

C_{ij}	Components of the material stiffness matrix
E_1, E_2	Young's modulus of the transversely isotropic plane
E_3	Young's modulus of the plane normal to the transversely isotropic plane
F	Applied normal force
G	Shear modulus
K	Bulk modulus
L, S	Barnett-Lothe tensor
M, N_f, N_m	Integers
$P(x)$	Pressure distribution
R	Radius of curvature of the parabolic cylinder
V	Volume fractions
$[a, b]$	Interval of the contact patch
f	Frictional coefficient
f, m, t	Subscripts expressing the matrix, fiber and transverse respectively
β	Anisotropic characteristic parameter
δ	Symmetry parameter
ν	Poisson's ratio

1. INTRODUCTION

Fiber reinforced polymer (FRP) composites are being increasingly used as alternatives for conventional materials mainly because of their high specific strength and specific stiffness. In addition, the self-lubricating properties of the composites render them suitable for applications like seals, bearings, gears and artificial prosthetic joints.

The FRP composite bearings are ideal for high load, low speed applications or where normal lubrication is difficult or costly. The composite bearings are used because of their advantages like self-lubrication, high load carrying capacity, increased life, lightweight, maintenance free, excellent dimensional stability, corrosion resistance and high temperature applications.

The fiber orientation has a significant influence on wear and friction behaviour of FRP composites. Sung and Suh [1], Cirino et. al. [2] and Viswanath et. al. [3] investigated that friction and wear behaviour of FRP composites vary with sliding directions. In these studies, the largest wear resistance was obtained when the sliding was normal to fiber orientation while the lowest wear resistance was found when fiber orientation was transverse to the sliding. For Epoxy/graphite composites, the friction coefficient was minimized when the orientation of the fibers was normal to the sliding surface. Conversely for Epoxy/Kevlar composites, the normal orientation was found to yield the highest friction.

For the purpose of fully utilizing the beneficial contact characteristics of FRP composites, it is necessary to obtain an in-depth knowledge of their contact behaviour. Hertzian and other fundamental contact theories are not valid for FRP composites due to their anisotropy. Fan and Hwu [4] have studied general contact problems for anisotropic elastic half-plane by combining analytical continuation and Stroh's formalism. Fan and Hwu [5, 6] have also derived a general closed-form solution for the sliding contact of bodies on anisotropic elastic planes.

This work attempts to apply Hwu and Fan's analytical solution to FRP composites in order to obtain a better understanding of their compliance behaviour. The frictional sliding contact between a unidirectional continuous FRP composite and a rigid parabolic cylinder is analysed based on the Hwu and Fan's solution. The influence of fiber ply orientation, fiber and matrix material combinations, the volume fraction of fiber, sliding direction and the friction coefficient on the contact pressure distribution and the contact area are ascertained and discussed. Further, optimum values of contact parameters are established to achieve maximum contact pressure using genetic algorithm.

2. PROBLEM FORMULATION

In this work, the unidirectional FRP composite bearing is modeled as quasi-homogeneous, transversely isotropic elastic half-plane that is in contact with an infinitely long, rigid parabolic cylinder. The sliding contact on anisotropic elastic half-plane has been derived using Hwu and Fan's closed form solution. A Cartesian co-ordinate system is defined such that Y-axis coincides with the vertical axis of the cylinder as shown in Fig. 1. The sliding direction is perpendicular to the axis of the cylinder and a motion occurs from left to right.

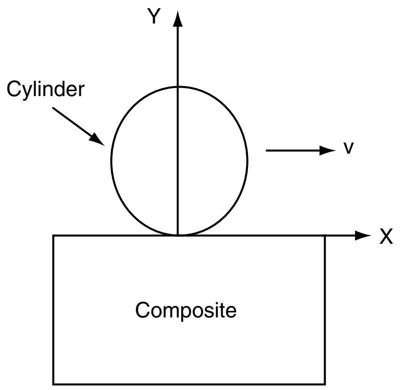

Figure 1. Contact model of a rigid cylinder on FRP composite.

2.1. Elastic properties of composites

When the co-ordinates coincide with the principal axes of the elastic half-plane, the stress-strain relationship of unidirectional composites can be described using five elastic constants. If X-Y plane is considered as transversely isotropic, the generalised Hook's law [7] becomes:

$$\begin{bmatrix} \sigma_1 \\ \sigma_2 \\ \tau_{12} \end{bmatrix} = \begin{bmatrix} C_{11} & C_{12} & 0 \\ C_{12} & C_{22} & 0 \\ 0 & 0 & C_{66} \end{bmatrix} \begin{Bmatrix} \varepsilon_1 \\ \varepsilon_2 \\ \gamma_{12} \end{Bmatrix} \tag{1}$$

The components of the stiffness may be expressed in terms of engineering constants

$$\begin{aligned} C_{11} &= \frac{E_1}{1-\nu_{12}\nu_{21}} \\ C_{12} &= \frac{\nu_{12}E_2}{1-\nu_{12}\nu_{21}} \\ C_{22} &= \frac{E_2}{1-\nu_{12}\nu_{21}} \\ C_{55} &= C_{66} = G_{12} \end{aligned} \tag{1a}$$

If the fiber is assumed to be isotropic, the elastic constants can be determined using the representative elastic properties of the fiber and the matrix as presented by Rosen [8] and Hashin [9]:

$$\begin{aligned} E_3 &= E_m V_m + E_f V_f + \frac{4V_m V_f (\nu_f - \nu_m)^2}{V_m/k_f + V_f/k_m + 1/G_m} \\ \nu_{31} &= E_m \nu_m + E_f \nu_f + \frac{V_m V_f (\nu_f - \nu_m)(1/k_m - 1/k_f)}{V_m/k_f + V_f/k_m + 1/G_m} \\ G_{12} &= G_m \frac{(\alpha + \beta_m V_f)(1+\rho V_f^3) - 3V_f V_m^2 \beta_m^2}{(\alpha - V_f)(1+\rho V_f^3) - 3V_f V_m^2 \beta_m^2} \\ E_1 &= E_2 = \frac{4k_t G_{12}}{k_t + G_{12}(1+4k_t \nu_{31}^2/E_3)} \\ \nu_{12} &= E_1/2G_{12} - 1 \\ \frac{E_i}{\nu_{ij}} &= \frac{E_j}{\nu_{ji}}; (i, j = 1, 2, 3) \\ k_t &= \frac{k_m k_t + (V_f k_f + V_m k_m)G_m}{V_m k_f + V_f k_m + G_m} \\ \alpha &= (\gamma + \beta_m)/(\gamma - 1) \\ k_f &= E_f/2(1-\nu_f - 2\nu_f^2); k_m = E_m/2(1-\nu_m - 2\nu_m^2) \end{aligned} \tag{2}$$

$$\begin{aligned} \beta_f &= 1/(3-4\nu_f); \beta_m = 1/(3-4\nu_m) \\ \rho &= (\beta_m - \gamma\beta_f)/(1+\gamma\beta_f); \gamma = G_f/G_m \\ f &= (V_f/f_f + V_m/f_m)^{-1} \end{aligned}$$

2.2. Frictional sliding contact pressure distribution

The two-dimensional sliding contact pressure on the anisotropic elastic half-plane has been obtained using Hwu and Fan's [6] closed-form solution.

$$P(x) = \frac{2\sin(\delta\pi)}{(\beta + \bar{\beta})}(b - x)^{\delta}(x + a)^{1-\delta} \tag{3}$$

$$\delta = \frac{1}{2\pi}\arg\left(\frac{-\bar{\beta}}{\beta}\right); 0 \le \delta \le 1 \tag{4}$$

$$a^2 = \frac{\delta(\beta + \bar{\beta})RF}{\pi(1-\delta)} \tag{5}$$

$$b^2 = \frac{(1-\delta)(\beta + \bar{\beta})RF}{\delta\pi} \tag{6}$$

Equations (3)-(6) describe the two dimensional contact of a parabolic cylinder on anisotropic elastic half-plane. The value of β can be determined as follows:

$$\beta = \frac{1}{L_{22}} - if\frac{S_{12}}{L_{22}} \tag{7}$$

The explicit expressions of L and S for orthotropic materials have been given in terms of the elastic components C_{ij} by Dongye and Ting [10] as follows:

$$S_{21} = \left(\frac{C_{66}\left(\sqrt{C_{11}C_{22}} - C_{12}\right)}{C_{22}(C_{12} + 2C_{66} + \sqrt{C_{11}C_{22}}}\right) \tag{8}$$

$$S_{12} = \frac{-\sqrt{C_{22}/C_{11}}}{S_{21}}; L_{11} = \left(C_{12} + \sqrt{C_{11}C_{22}}\right)S_{21} \tag{9}$$

$$L_{22} = \frac{\sqrt{C_{22}/C_{11}}}{L_{11}}; L_{33} = (C_{44}C_{55})^{1/2} \tag{10}$$

It is important to note that the parameters of β and δ reflect the degree of anisotropy properties and the amount of friction respectively. For a smooth surface, the value of δ is 0.5 and the contact profile is symmetrical about the vertical axis of the parabolic cylinder. For surfaces with friction, the contact patch becomes asymmetrical. The value of δ describes the deviation of the maximum contact pressure from the axis of the parabolic cylinder. If the value of δ is less than 0.5, the maximum normal pressure deviates to the side of the moving direction. If δ is larger than 0.5, the maximum normal pressure would deviate in the opposite direction. Usually, the value of δ is less than 0.5, and hence the absolute value of '*b*' is larger than that of '*a*' in the contact patch.

3. SENSITIVITY ANALYSIS

Based on the representations of elastic properties of FRP composites (Eq.(1)), law of mixture and the analytical solutions (Eqs. (3)–(6)), the influence of material combinations, fiber ply orientation, fiber volume fraction and sliding direction on the contact pressure distributions of FRP composite bearing can be determined. Here, a normal force of 1 N and an indent radius of 8 mm is considered. Three different sliding directions are considered: (1) Transverse direction (TL); (2) Normal direction (NL) and (3) Parallel direction (PL), which are illustrated in Fig. 2.

The pressure distributions for a wide range of contact conditions are plotted in Figs. (2)–(7). In these figures, the horizontal co-ordinate is marked according to the fraction of the average contact half-width, x_0.

$$x_0 = (a_1 + b_1)/2 \tag{11}$$

In Eq.(9), (a_1, b_1) represents the interval of the contact patch. The vertical co-ordinate represents the pressure values.

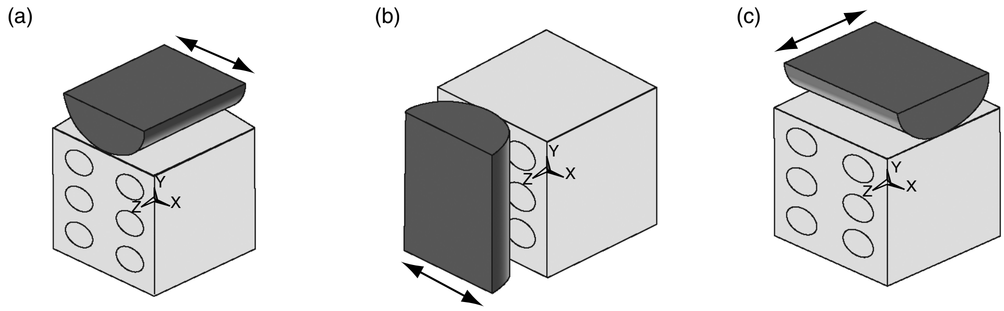

Figure 2. Fiber orientation and the sliding directions (a) Transverse (b) Normal (c) Parallel.

3.1. Influence of sliding direction

The influence of the sliding direction is shown in Fig. 3 for Aramid/Epoxy composite. It is found that the contact pressure distribution and the contact patch can significantly vary with the sliding directions. In this figures, the largest maximum pressure and the smallest contact patch occur in the normal sliding direction [1, 11]. There is only a slight variation in the contact pressure between the transverse and parallel directions. The maximum contact pressure in the normal direction deviates the farthest distance from the vertical axis of the cylinder and is nearest to the vertical axis of the cylinder in the case of the transverse and parallel directions. This is due to the fact that the normal direction is very stiff and has a small contact area than the other two directions.

3.2. Influence of fiber material

The fibers of FRP composites give them their unique mechanical characteristics. Figures 4(a)–4(c) illustrate the variation of the contact pressure distributions of four different fiber materials in the transverse, normal and parallel sliding directions respectively. The fiber materials and their properties are given in Table 1. It is important to note that the matrix material is identical for all the results in Figures 4(a)–4(c). Here the fiber volume fraction of 60% is considered.

From the figures, it is found that the fiber material has little influence on the contact profile and magnitude of the pressure in the transverse direction. The contact pressure increases from 7.69 MPa for the glass fiber to 7.73 MPa for carbon fiber and there is negligible change in the area of the contact patch. The symmetry parameter δ increases from 0.4612 for the glass fibers to 0.4894 for the carbon fibers.

In the results of the parallel direction, it is similarly found that the fiber material has little effect on the profile and magnitude of the pressure. The maximum pressure increases from 7.53 MPa to 7.56 MPa for the glass and carbon fibers respectively. The value of δ increases from 0.4628 to 0.4898 for the glass and carbon fibers respectively. This shows that the contact profile becomes more symmetric and decreases in magnitude with increase in fiber elastic modulus.

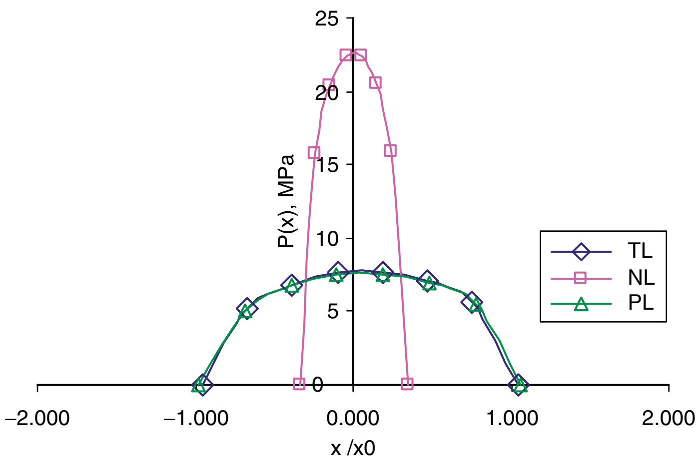

Figure 3. Pressure distribution for Aramid/Epoxy in three sliding directions.

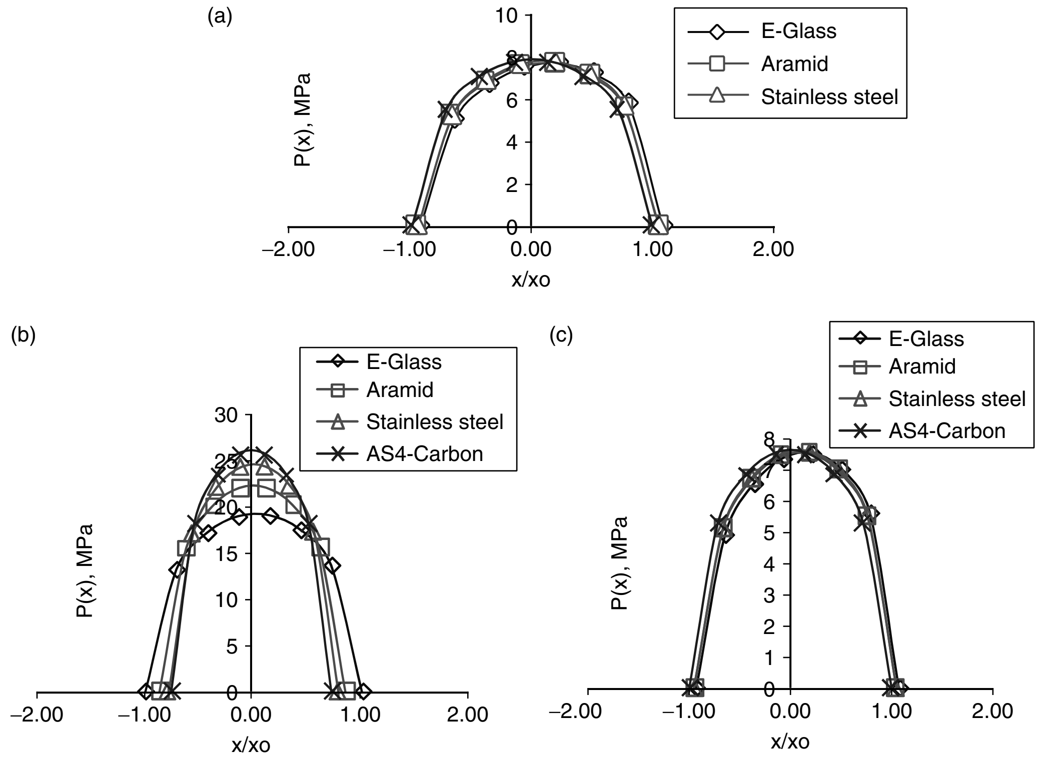

Figure 4. Pressure distribution for E-Glass, Aramid, Stainless steel and AS4 carbon fibers (a) Transverse (b) Normal (c) Parallel.

Table 1. Material properties

Material	Modulus GPa	Poisson's ratio	Frictional coefficient
E-Glass	72	0.2	0.43
Aramid	130	0.36	0.17
Stainless steel	186	0.3	0.18
AS4 - Carbon	235	0.2	0
Epoxy	0.33	0.34	0.3
PEEK	3.6	0.3	0.4

In the normal direction, the contact profile and pressure vary significantly with fiber materials. The contact width considerably narrows and the maximum pressure sharply increases with the longitudinal elastic modulus of the fiber. In these figures, the maximum pressure varies from 19.27 MPa for the glass fiber to 25.98 MPa for the carbon fiber. The symmetry parameter changes from 0.4904 to 0.4985 for the glass and carbon fibers respectively. This shows that the contact traction in the normal direction has significant sensitivity to the variation of the fiber material properties. This tendency is due to the fact that the fibers carry a significantly larger portion of the load in the normal direction than in the transverse and parallel directions.

3.3. Influence of fiber volume fraction

The fiber volume fraction is important parameter in determining the stiffness characteristics of composites. This is due to the fact that the engineering properties of composites are often dominated by the mechanical and physical properties of the fiber reinforcements. Since the fiber material is stiffer than its matrix counterpart, increasing the fiber volume fraction will substantially decrease its compliance.

Figures 5(a)–5(c) illustrate the influence of fiber volume fraction on the pressure distribution for Aramid/Epoxy composite. Here the fiber volume fraction was varied between 0.4 and 0.7. The fiber volume fraction has considerable influence on the contact pressure distribution. As the fiber volume

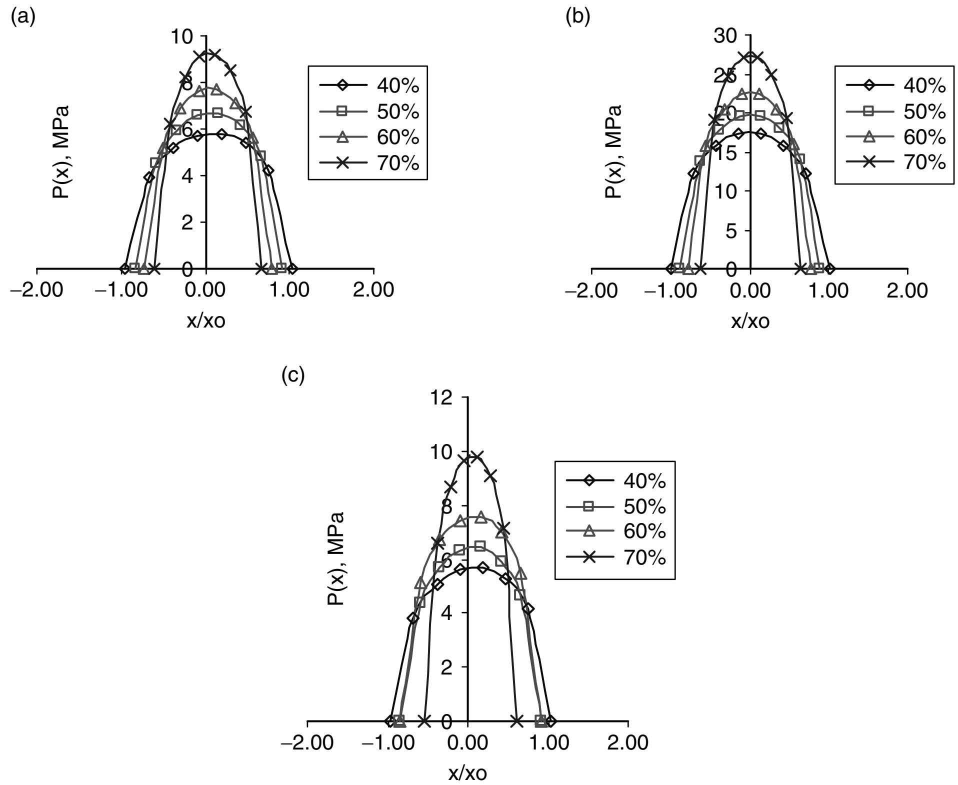

Figure 5. Pressure distribution with variation of fiber volume fraction for Aramid/Epoxy (a) Transverse (b) Normal (c) Parallel.

fraction increases from 0.4 to 0.7, the maximum pressure for all the three sliding directions shows a considerable increase [1, 11]. The contact distribution becomes less symmetric as the fiber volume fraction increases.

It is found that in the normal direction $\delta = 0.4968$, 0.4966, 0.4965 and 0.4958 for the volume fraction of 0.4, 0.5, 0.6 and 0.7 respectively. However it is important to note that there are limits on the magnitude of fiber volume fraction, as the matrix volume fraction must be sufficient to satisfy its bonding and protective functions.

3.4. Influence of matrix materials

Polymer resins serve as the bonding and protective agent. The matrix material is an important parameter in determining the contact behavior of FRP composites. Figures 6(a)–6(c) show the influence of the matrix material on the pressure distribution. In these figures, the composites consist of E-Glass fibers with a volume fraction of 60%.

From the figures, it is seen that the matrix material has a great influence on the contact pressure distribution. The maximum pressure increases by 300% in the transverse and parallel directions when the matrix material is changed from Epoxy to PEEK (Polyether ether ketone). This is clearly due to the fact that the PEEK resin (E = 3.6 Gpa) is stiffer than the Epoxy (E = 0.33 Gpa) and has lesser compliance as indicated by the smaller contact areas. The value of δ is moderately larger ($\delta_{TL} = 0.4612$, $\delta_{NL} = 0.4904$, $\delta_{PL} = 0.4628$) for Epoxy than for the stiffer PEEK ($\delta_{TL} = 0.4550$, $\delta_{NL} = 0.4811$, $\delta_{PL} = 0.4543$). But in the case of normal direction, the maximum pressure increases less than 100% between the Epoxy and PEEK matrix materials.

3.5. Influence of fiber ply orientation

The influence of fiber ply orientation on the maximum contact pressure, contact patch and symmetry parameter is shown in Figures 7(a)–7(c) for Epoxy/E-Glass composite. A fiber volume fraction of 60% is considered and fiber ply orientation is varied from 0° to 90°.

From the figures, it is seen that the maximum pressure remains constant in the transverse and parallel directions. This shows that the fiber ply orientation has no effect on the contact pressure

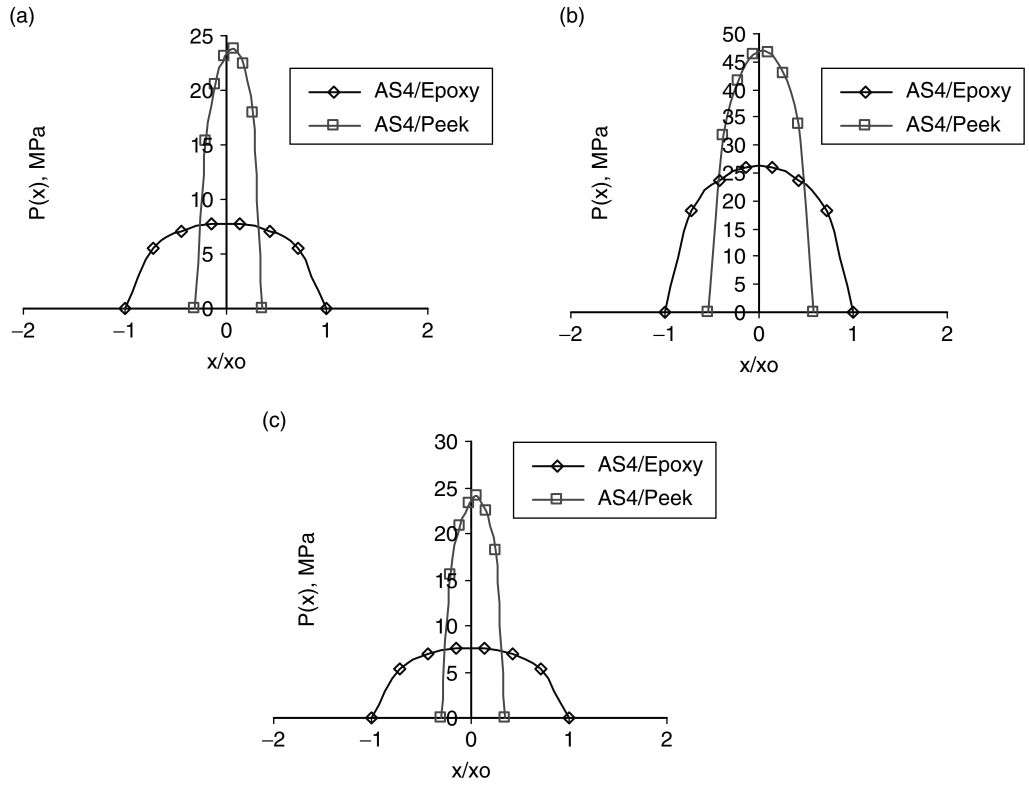

Figure 6. Pressure distribution for AS4/Epoxy and AS4/PEEK (a)Transverse (b) Normal (c) Parallel.

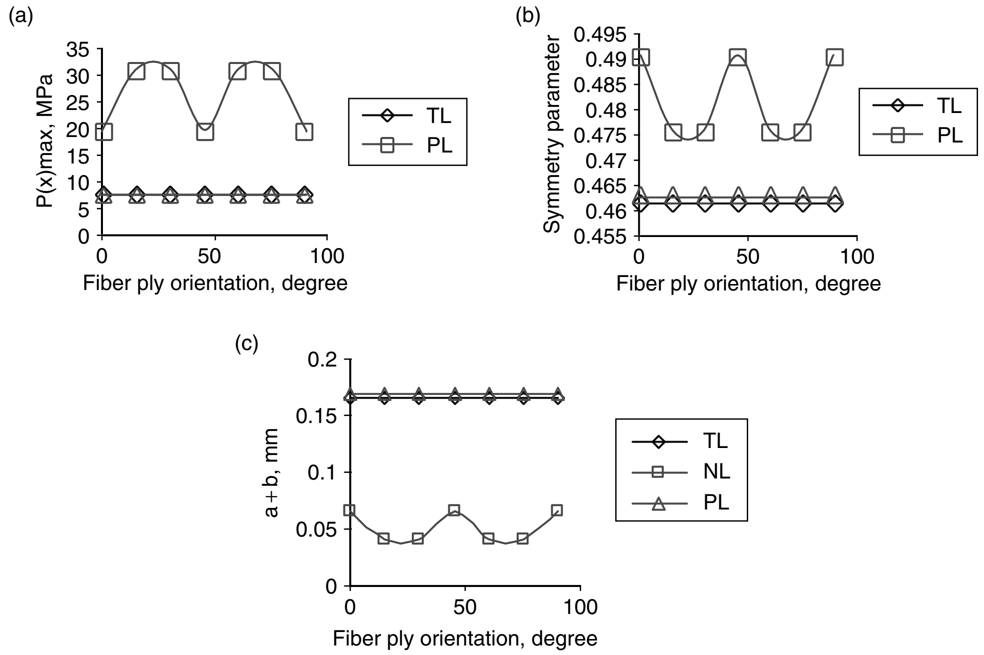

Figure 7. Variation of maximum pressure P_{max}, symmetry parameter δ and contact patch width a + b with fiber ply orientation.

distribution in these two directions. But the maximum pressure varies with increase in the fiber ply orientation in the normal direction. The contact pressure is maximum at two values of ply orientation (22.5° and 67.5°). It is also seen from the figures that the symmetry parameter δ and the contact patch remain constant for the transverse and parallel directions. In the case of normal direction, the value of δ and the contact patch varies significantly with increase of the fiber ply orientation. The value of δ and the contact patch are minimum at 22.5° and 67.5°. This shows that the fiber ply orientation has influence only in the normal direction. This is due to the fact that the fibers carry significantly larger portion of the load in the normal direction than in the transverse and parallel directions.

4. OPTIMIZATION OF CONTACT PARAMETERS

It is found from the equations (3)–(10), that the contact pressure depends on sliding direction (M), Young's modulus of fiber (E_f), fiber volume fraction (V_f), Young's modulus of matrix (E_m), applied normal force (F), radius of curvature of the parabolic cylinder (R) and fiber ply orientation (θ).

In this work, three sliding directions, four fiber materials, fiber volume fraction of 40% to 70%, two matrix materials and fiber ply orientation of 0 to 90 degrees are considered. A normal force of 1 N and radius of 8 mm is assumed. Hence the contact pressure is taken as a function of M, E_f, V_f, E_m and θ. The values of E_f and E_m are related to fiber material number (N_f) and matrix material number (N_m). Genetic algorithm (GA) [12] is used for optimization of the contact parameters with the objective of maximizing the contact pressure.

The values assigned to M, N_f and N_m and the corresponding material properties are given in Table 2 – Table 4. In GA, all the variables are expressed by strings of bits. The values of different variables and corresponding number of bits required for binary representation are given in Table 5. Thus a total of nineteen bits were required to represent an input string i.e. string length is equal to 19. Thus, the objective function has a solution space of size 2^{19} = 5, 24, 288.

The genetic operators, namely reproduction, crossover and mutation are applied to the strings of length 19, for the process of optimization. The crossover carried out here is three-point-crossover with 100% probability. The mutation is carried out with 3% probability. The population size is considered to be 50, with 50 population generations. Hence with the technique of genetic algorithm, the total number of objective function value-calculations is reduced to 2,500 (50 × 50) from the space of 2^{19}. The processes in GA are explained in Fig. 8.

Table 2. Values of *M*

M	**0**	**1**	**2**
Sliding Direction	Transverse	Normal	Parallel

Table 3. Values of N_f and Material Properties

N_f	**0**	**1**	**2**	**3**
Fiber material	E-Glass	Aramid	Stainless steel	AS4-Carbon
Modulus (GPa)	72	130	186	235
Poisson's ratio	0.2	0.36	0.3	0.2
Friction coefficient	0.43	0.17	0.18	0

Table 4. Values of N_m and Material Properties

N_m	**Matrix material**	**Modulus (GPa)**	**Poisson's ratio**	**Friction coefficient**
0	Epoxy	0.33	0.34	0.3
1	PEEK	3.6	0.3	0.4

Table 5. Values of Variables and Number of Bits Considered

Variables	M	N_f	V_f	N_m	θ
Range of values	0, 1, 2	0, 1, 2, 3	40%–70%	0, 1	0–90
No. of bits considered	2	2	7	1	7

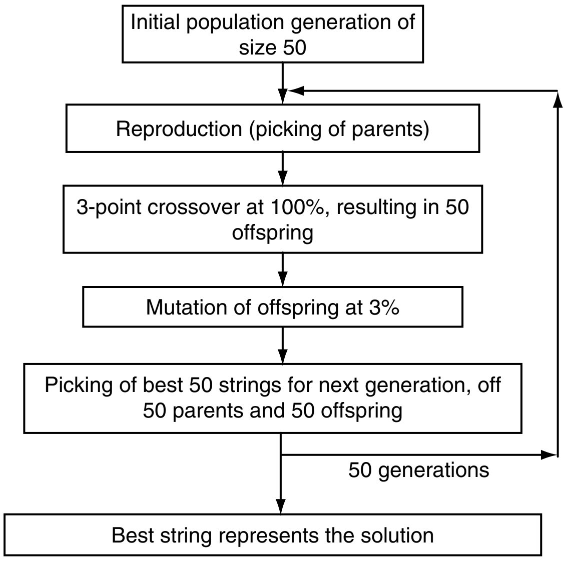

Figure 8. Steps in GA.

The objective function and constraints are given below:

$$\text{Maximize} \quad P = \frac{2\sin(\delta\pi)}{(\beta+\bar{\beta})}(b)^{\delta}(a)^{1-\delta}$$

$$\begin{aligned} \text{where} \quad P &= f(M, E_f, V_f, E_m, \theta) \\ &= f(M, N_f, V_f, E_m, \theta) \end{aligned}$$

subject to the constraints

$$0 \le M \le 2; \qquad 0 \le N_f \le 3; \qquad 0.4 \le V_f \le 0.7; \qquad 0 \le N_m \le 1; \qquad 0 \le \theta \le 90;$$

The optimum values of contact parameters obtained from the GA are given in Table 6. The results obtained from GA showed that the normal direction has more wear resistance because the fibers are carrying larger portion of the load in that direction. In the case of material combinations, the materials with higher elastic modulus contribute more to the contact pressure. If the volume fraction of the fiber is more, the contact pressure is also high. The contact pressure is maximum at two values of fiber ply orientation i.e. 22.5° and 67.5°. Instead of studying the influence of contact parameters independently, the GA gives the optimum values of the contact parameters.

Table 6. Results of GA

Contact parameter	Optimum value
Sliding Direction (M)	2 (Normal)
Fiber Material (N_f)	3 (AS4-Carbon)
Volume Fraction (V_f)	70%
Matrix Material (N_m)	1 (PEEK)
Fiber Ply Orientation (θ)	22.5° and 67.5°
Contact Pressure (P_{max})	67.21 MPa

5. CONCLUSIONS

The influence of fiber ply orientation, fiber and matrix material combinations, the volume fraction of fiber and sliding direction on the contact pressure distribution and the contact area for unidirectional continuous FRP composite bearing have been evaluated by applying Fan and Hwu's closed form solution. The findings are summarised below:

- The highest maximum contact pressure is obtained in the normal sliding direction. This is due to the fact that the fibers are carrying a large proportion of the load.
- The analytical results indicate that the contact pressure and contact patch play an important role in the wear of FRP composites. This is similar to the results found by the experiments [1, 2, 10]; the normal direction possesses the highest wear resistance.
- The contact pressure distribution is not symmetrical. The normal sliding direction has the least symmetric contact area, whereas the parallel direction has the most symmetric area.
- The contact pressure in the transverse and parallel directions show little change, whereas significant influence is there in the normal direction with the variation of fiber materials because the fibers carry a large proportion of the load in the normal direction.
- Since the fibers are stiffer than the matrix materials, increasing the volume fraction of fibers increases the maximum contact pressure in all the three sliding directions.
- The maximum contact pressure varies significantly with the elastic modulus of the matrix materials. The normal direction is the least sensitive to changes in the matrix materials.
- The transverse and parallel directions are least sensitive to the fiber ply orientation, whereas the normal direction shows a considerable change in the maximum contact pressure, contact patch and symmetry parameter with a variation of the fiber ply orientation.
- The results obtained from GA showed that the normal direction has more wear resistance because the fibers are carrying larger portion of the load in that direction.
- In the case of material combinations, the materials with higher elastic modulus contribute more to the contact pressure.
- If the volume fraction of the fiber is more, the contact pressure is also high.

REFERENCES

[1] Sung, N. H., and Suh, N. P., 1978, "Effect of Fiber Orientation on Friction and Wear of Fiber Reinforced Polymeric Composites", Wear, 53, pp. 129–141.

[2] Cirino, M., Friedrich. K., and Pipes, R.B., 1988, "The Effect of Fiber Orientation on the Abrasive Wear Behaviour of Polymer Composite Materials", Wear, 121, pp. 127–141.

[3] Viswananth, B., Verma, A. P., and Rao, V. S. K., 1993, "Effect of Reinforcement on Friction and Wear of Fabric Reinforced Polymer Composites", Wear 167, pp.93–99.

[4] Fan, C. W., and Hwu, C., 1996, "Punch Problems of Anisotropic Elastic Half-Plane", ASME J. Appl. Mech., 63, pp. 69–76.

[5] Hwu, C., and Fan, C. W., 1998, "Contact Problems of Two Dissimilar Anisotropic Elastic Bodies", ASME J. Appl. Mech., 65, pp. 580–587.

[6] Hwu, C., and Fan, C. W., 1998, "Sliding Punches With or Without Friction Along the Surface of Anisotropic Elastic Half-Plane", Q. J. Mech. Appl. Math., 51, pp. 159–177.

[7] Autar K. Kaw., 1997, Mechanics of Composite Materials, CRC Press.

[8] Rosen, B. W., 1973, "Stiffness of Fiber Composite Materials", Composites, 4, pp. 16–25.

[9] Hashin, Z., 1983, "Analysis of Composite Materials - A Survey", ASME J. Appl. Mech., 50, pp. 481–505.

[10] Dongye, C., and Ting, T. C. T., 1989, "Explicit expressions of Barnett-Lothe Tensors and Their Associated Tensors for Orthotropic Materials", Q. J. Mech. Appl. Math., 47, pp. 724–734.

[11] Tsukizoe, T., and Ohmae, N., 1986, "Friction and Wear Performance of Unidirectional Fiber Reinforced Polymer Composites", Elsevier, New York, pp. 205–231.

[12] Rao, S. S., 1996, "Engineering Optimization: Theory and Practice", John Wiley & Sons Ltd.